

# Amplifying the Macromolecular Crowding Effect Using Nanoparticles

Ahmed Zaki, Neeshma Dave, and Juewen Liu\*

Department of Chemistry, Waterloo Institute for Nanotechnology, University of Waterloo, Waterloo, Ontario N2L 3G1, Canada

**S** Supporting Information

**ABSTRACT:** The melting temperature ( $T_m$ ) of DNA is affected not only by salt but also by the presence of high molecular weight (MW) solutes, such as polyethylene glycol (PEG), acting as a crowding agent. For short DNAs in a solution of low MW PEGs, however, the change of excluded volume upon melting is very small, leading to no increase in  $T_m$ . We demonstrate herein that by attaching 12-mer DNAs to gold nanoparticles, the excluded volume change was significantly increased upon melting, leading to increased  $T_m$  even with PEG 200. Larger AuNPs, higher MW PEGs, and higher PEG concentrations show even larger effects in stabilizing the DNA. This study reveals a unique and fundamental feature at nanoscale due to geometric effects. It also suggests that weak interactions can be stabilized by a combination of polyvalent binding and the enhanced macromolecular crowding effect using nanoparticles.

Macromolecules such as proteins, RNA, and DNA occupy 20–40% of a live cell's volume.<sup>1</sup> Due to their mutually impenetrable nature, the excluded volume occupied by each macromolecule is larger than its geometric volume, making the addition of new polymers into this crowded system thermodynamically disfavored. This fundamental biophysical effect has a strong influence on many biochemical reactions, including protein folding, oligomerization, and DNA hybridization and melting.<sup>2</sup> Much attention has been given to the process of DNA melting, which is important in biology and biotechnology.<sup>3–8</sup> At the same time, DNA length and sequence can be easily varied to allow systematic studies.

Upon melting, the excluded volume of a DNA is increased. Therefore, melting is usually disfavored in macromolecularly crowded environments to give rise to more stable DNA duplex and increased melting temperature ( $T_m$ ). Polyethylene glycol (PEG), the most commonly used crowding agent, has been shown to both stabilize and destabilize DNA, depending on PEG molecular weight (MW), DNA length, and salt concentration. For example, with 8–17 base pair (bp) DNAs in the presence of 1 M NaCl, only destabilization (reduced  $T_m$ ) was observed even with 20% PEG 8000.<sup>7</sup> By reducing the salt to 100 mM, stabilization of a 20 bp DNA was observed with 15% PEG 6000.<sup>5</sup> On the other hand, with ~200 bp DNAs, an increase in  $T_m$  was achieved for PEG MW > 400–1000.<sup>4</sup> This is because, under otherwise identical conditions, longer DNAs produce larger excluded volume increases upon melting. The fact that decreased  $T_m$  was also sometimes observed suggests that PEGs play a dual role in DNA stability. In addition to the excluded volume effect for stabilization, PEGs also reduce the

water activity and solvate DNA bases, leading to decreased  $T_m$ .<sup>4,5,7</sup> In this paper, macromolecular crowding (MC) describes solely the excluded volume effect, while the chemical interaction between PEG and DNA is called the destabilizing chemical effect. Efforts to dissect these two effects have been recently carried out. In general, small PEGs tend to have a strong destabilizing chemical effect and weak MC effect, leading to an overall reduced  $T_m$ .<sup>8</sup>

Based on the understanding of excluded volume, we consider that attaching short DNAs to a larger object, such as a gold nanoparticle (AuNP), might augment the excluded volume change upon DNA melting and thus amplify the MC effect. This hypothesis is supported by a simple geometric calculation that will be discussed later. Since the first report in 1996,<sup>9,10</sup> DNA-linked AuNPs are among the most well-studied systems in bionanotechnology,<sup>11,12</sup> with many unique properties, including a blue-to-red color change upon melting and a sharp melting transition. The melting of such DNA-linked AuNPs in high MW PEGs (MW > 8000) with 300 mM NaCl has been reported to be qualitatively similar in the presence or absence of AuNPs.<sup>13</sup> We consider that, with such high MW PEGs and salt, even free DNAs were effectively stabilized, and the role of AuNPs might have been masked.<sup>8</sup> Herein, we focus on low MW PEGs in low salt conditions. We report for the first time that the  $T_m$  of AuNP-attached DNA was increased in the presence of even PEG 200, while free DNAs still showed reduced  $T_m$ . The  $T_m$  increase positively correlated with AuNP size, supporting that AuNPs can amplify the MC effect.

We functionalized 13 nm AuNPs with two kinds of thiol-modified 12-mer DNA and assembled them using a 24-mer linker DNA. The temperature of the sample was gradually increased to induce DNA melting and AuNP disassembly (Figure 1A).<sup>11</sup> Since the melting of either 12-mer DNA can induce AuNP disassembly, a 12-mer DNA duplex in the absence of AuNPs was also prepared (Figure 1B). To achieve high precision and high throughput in  $T_m$  measurement, these free DNAs were labeled with a fluorophore and quencher, respectively, and a real-time PCR thermocycler was used to obtain melting curves. This fluorescence method was previously reported,<sup>14</sup> and a comparison to the tradition method based on the UV hyperchromic effect was recently carried out.<sup>15</sup> Based on this report, our fluorescent DNA should give precise and accurate  $T_m$  results.

The melting curves of the AuNP-free fluorescent DNA in water, 5% (w/w) glycerol, ethylene glycol (EG), or PEGs of different MWs are shown in Figure 2A. All the solutions also contained 50 mM NaCl, 10 mM HEPES, pH 7.6. The

Received: August 13, 2011

Published: December 14, 2011

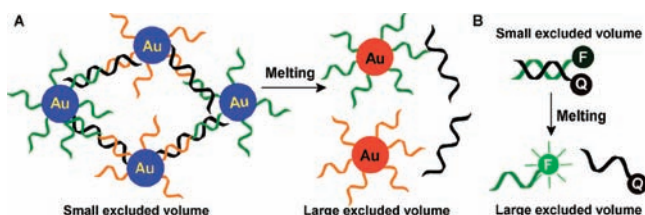


**Figure 1.** Schematic presentation of the melting of DNA-linked AuNPs (A) and the melting of free DNA based on fluorescence (B). The increase of excluded volume upon melting is much larger in (A) than in (B). The crowding agent (PEG) is not drawn.

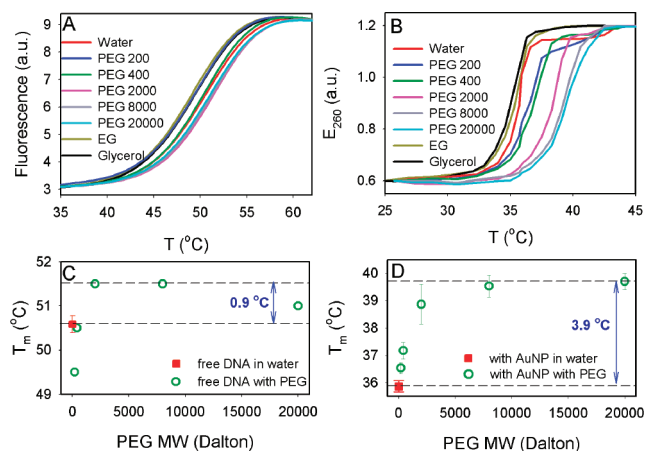


**Figure 2.** Melting curves of the free DNA (A) and the DNA-linked 13 nm AuNPs (B) in 5% (w/w) solutes. The melting buffer contained 50 mM NaCl, 10 mM HEPES, pH 7.6.  $T_m$  as a function of PEG MW for the free DNA (C) and the DNA-linked 13 nm AuNPs (D). The samples in the absence of any PEG are shown in red. The two dashed lines define the maximal stabilization by 5% PEG. The error bars represent the standard deviations of independent measurements.

fluorescence intensity gradually increased with increasing temperature, indicating DNA melting. The sample in water was measured 12 times, and the coefficient of variation was only 0.4% (Figure 2C, red square), supporting the outstanding reproducibility of fluorescence measurement. Glycerol and EG, as well as PEG 200, destabilized the DNA, while PEG 2000 and above stabilized it.  $T_m$  as a function of PEG MW is shown in Figure 2C. Compared to the sample in water (red square), the  $T_m$  decreased  $\sim 1.2$  °C in PEG 200. PEG 2000, 8000, and 20000 stabilized the duplex but only for  $\sim 0.9$  °C (dashed lines in Figure 2C), consistent with literature reports that the stabilization effect was very small for short DNAs.<sup>7</sup>

Record and co-workers recently reported that small PEGs had stronger destabilizing chemical effects than the excluded volume interaction, resulting in reduced  $T_m$ .<sup>8</sup> On the other hand, high MW PEGs had strong excluded volume stabilization while the destabilizing chemical interaction was attenuated since a large fraction of the PEG chains were shielded. The transition to an overall stabilization occurred at PEG 400, and PEGs larger than 2000 did not show further stabilization in the presence of the same PEG monomer unit concentration (i.e., w/w concentration). Our observations in Figure 2C are in good agreement with this report and thus can be explained by their model.

Next the melting curves of DNA-linked 13 nm AuNPs were measured. Representative TEM micrographs and UV/vis spectra of these AuNPs are presented in Supporting

Information (SI). The AuNP extinction at 260 nm was monitored as a function of temperature (Figure 2B). Melting with AuNPs occurred in a much narrower temperature range, which is characteristic of such polyvalent DNA binding systems undergoing cooperative melting transitions.<sup>16</sup> Interestingly, all of the PEGs induced stabilization in the presence of AuNPs, even for PEG 200, while small-molecule solutes (glycerol and EG) still showed reduced  $T_m$ , suggesting the important role of the MC effect acting on the AuNPs. The excluded volume interaction with AuNPs must be so large that it overcompensated the destabilizing chemical effect of PEG 200 on the DNA. This is the first time that an increase in duplex DNA  $T_m$  was observed for such small PEGs and short DNA,<sup>5,17</sup> highlighting the crucial role of AuNPs. With higher MW PEGs, a  $T_m$  increase to 3.9 °C was achieved (Figure 2D), which was more than 4-fold that for the free DNA. In this regard, the MC effect was amplified by the presence of AuNPs.

So far, we have demonstrated an amplified stabilization effect by confining DNA at the surface of 13 nm AuNPs. Next, we aim to test the effect of AuNP size. For this purpose, we prepared 5, 13, 20, and 30 nm AuNPs functionalized with the same DNAs. Their melting curves were measured in 10% PEG 200. Stabilization was observed even with 5 nm AuNPs (Figure

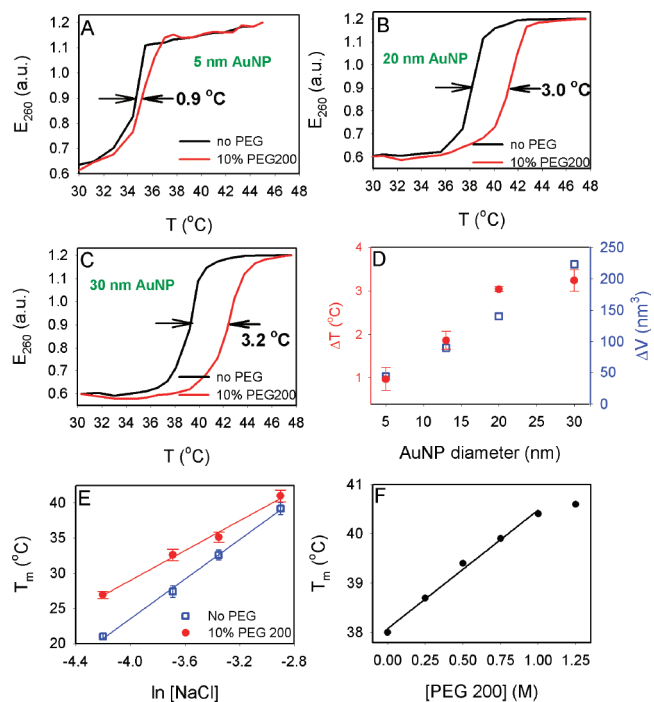


**Figure 3.** Melting curves of DNA-linked AuNPs: (A) 5, (B) 20, and (C) 30 nm in the presence and absence of 10% PEG 200. (D) Increase of  $T_m$  (red dots, left axis) and calculated increase of the excluded volume (blue squares, right axis) as a function of AuNP size. (E) Effect of NaCl concentration on  $T_m$ . The x-axis is the natural logarithm of [NaCl] in molar. (F) Effect of PEG concentration on  $T_m$  of 13 nm AuNPs. 1 M PEG 200 is  $\sim 20\%$  (w/w).

3A), although the  $T_m$  shift was only  $\sim 0.9$  °C. Very large  $T_m$  shifts exceeding 3 °C were achieved with 20 and 30 nm AuNPs (Figure 3B,C). The  $T_m$  increase is plotted as a function of AuNP size in Figure 3D (red dots); larger AuNPs produced a higher increase in  $T_m$ .

With a high density of polyanionic DNA, these AuNPs are known to enhance the local cation concentration, which

stabilizes duplex DNA.<sup>14,18</sup> The effect of salt on DNA melting,<sup>19</sup> especially in a crowded environment, has been carefully studied.<sup>4–6</sup> To understand whether the presence of AuNPs can affect the association of salt with DNA in such a crowded environment, we measured the  $T_m$  of AuNPs as a function of NaCl concentration. A linear relationship was obtained in both the presence and absence of 10% PEG 200 (Figure 3E), typical for DNA melting. The slope of these curves is proportional to the number of sodium ions bound to DNA upon duplex formation or released upon melting.<sup>4–6</sup> A smaller slope was observed in the presence of PEG, suggesting that PEG reduced the number of  $\text{Na}^+$  associated with DNA upon forming AuNP aggregates, similar to the behavior of free DNA.<sup>4–6</sup> Figure 3E also shows that the  $T_m$  shift was larger in lower salt buffers. For example, with 15 mM NaCl, 10% PEG 200 was able to increase  $T_m$  by  $\sim 6^\circ\text{C}$  for the 13 nm AuNPs. This property has also been reported for free DNA, in which the crowding effect was more pronounced for weak interactions.<sup>4–6</sup> Therefore, the presence of AuNPs did not change the interaction between salt and DNA.

We rationalize our observations on the basis of the model shown in Figure 4A. If only two AuNPs are linked by DNA to

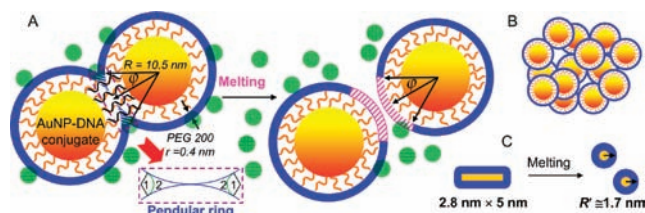


**Figure 4.** (A) Schematics of excluded volume change after melting of a DNA-linked AuNP dimer (13 nm AuNP in PEG 200). The blue solid lines enclose the excluded volumes. The regions of interest for calculating excluded volume increase form a pendular ring (shaded) and are defined by the  $\varphi$  angle. This pendular ring prior to melting is divided into parts 1 and 2 for volume calculation (see SI). After melting, the same regions are shaded in pink. (B) There are multiple neighbors for each AuNP, producing an even larger increase in the excluded volume upon melting. (C) Schematics of excluded volume change for a 12-mer duplex upon melting. The dimensions are estimated on the basis of zero excluded volume change. Drawings are not to scale.

form a dimer and PEGs cannot penetrate through the DNA layer, the excluded volume of this dimer is the volume encased by the blue solid line. The thickness of this line is determined by the size of PEG,  $\sim 0.4$  nm for PEG 200 (i.e., the hydrodynamic radius).<sup>20</sup> Here, PEG is treated as a hard sphere (e.g., green spheres in the figure), and its center is excluded from the blue line. Therefore, the excluded volume becomes much larger with high MW PEGs. In the absence of PEG, the excluded volume is the same as the geometric volume, and there is no crowding effect. By treating PEGs as hard spheres, we assumed that they were in the dilute regime; this is supported by the fact that the onset of chain overlap occurs at  $\sim 33\%$  for PEG 200,<sup>21</sup> much higher than the 5–10% concentration range used in this work.

After melting, the excluded volume increases, originating only from the pendular ring between the two AuNPs, as the rest is not affected by melting. The volume of the pendular ring before melting is given by  $V_p = F(R, \varphi)$ , where  $R$  is the radius of the DNA-functionalized AuNP,  $\varphi$  is the angle related to the PEG and AuNP size, and  $\varphi$  defines the boundary of the

pendular ring (i.e., PEG is excluded from the volume within the  $\varphi$  angle). For 13 nm AuNPs in the presence of PEG 200, this pendular volume is calculated to be  $10.7 \text{ nm}^3$ . After melting, the new excluded volume from this region is calculated to be  $101 \text{ nm}^3$ , an increase of  $90.3 \text{ nm}^3$ . If the AuNP size is increased to 30 nm, the increase of the excluded volume reaches  $223 \text{ nm}^3$ , which is consistent with our observation that the  $T_m$  shifts more for larger AuNPs. The calculated excluded volume change is plotted as a function of AuNP size in Figure 3D (blue squares), and a roughly linear relationship is observed. The change of  $T_m$ , however, is not linear (red dots). The model presented here is an idealized geometric model with a number of assumptions and simplifications. It does not consider the DNA conformational change upon melting, the number of DNA linkages between AuNPs, or the excluded volume of the linker DNA. Building a more precise model will be a subject of future studies. The detailed geometric deduction of the current model is included in SI.

So far, we only considered the melting of two AuNPs. The excluded volume change is further amplified if we consider that each AuNP aggregate contains hundreds to thousands of AuNPs and each AuNP can be in contact with up to 12 others in a close-packed form. Therefore, on a per particle basis, the above calculated excluded volume increase should be multiplied by a factor up to 6.<sup>22,23</sup> It is known that under our experimental conditions the packing of AuNPs was likely to be noncrystalline and fractal (Figure 4B),<sup>24</sup> giving a factor smaller than 6.

Above, we fixed the PEG MW = 200 and varied the AuNP size. In the following, the AuNP size is fixed and PEG MW and concentration are varied. The following equation describes the change of melting temperature  $\Delta T_m$  due to the excluded volume change  $\Delta V_{\text{ex}}$  upon DNA melting:<sup>4</sup>

$$\Delta T_m = \left( RT_m^0 / \Delta H \right) \Delta V_{\text{ex}} C_p \quad (1)$$

where  $R$  is the gas constant,  $\Delta H$  the enthalpy of DNA melting,  $T_m^0$  the  $T_m$  in the absence of PEG, and  $C_p$  the molar concentration of PEG. Equation 1 predicts a linear relationship between  $\Delta T_m$  and  $C_p$ . We performed PEG 200 concentration-dependent  $T_m$  measurements using 13 nm AuNPs. A linear relationship was indeed observed (Figure 3F), further confirming that the MC effect was taking place even with AuNPs. The original melting traces and also the melting of 30 nm AuNPs are presented in SI.

Usually  $\Delta H$  does not change much in the presence of PEG.<sup>5,8,25</sup> Therefore for PEGs of different MW,  $\Delta T_m$  is mainly determined by  $\Delta V_{\text{ex}}$  and  $C_p$ . According to our geometric model, higher MW PEGs should give rise to larger  $\Delta V_{\text{ex}}$ . We estimated  $\Delta V_{\text{ex}}$  for a 13 nm AuNP dimer with PEG 2000 and 8000 to be 492 and  $1917 \text{ nm}^3$ , respectively. With a concentration of 5% (w/w), the molar concentration of PEG 8000 was only a quarter of that of PEG 2000. The fact that they had a similar  $\Delta T_m$  in Figure 2D also supported our geometric model.

Even with AuNPs, the destabilizing chemical effect can still act on DNA. This can be concluded from the reduced  $T_m$  in the presence of glycerol and EG. Because free DNA melting is a fully reversible and two-state process, Record and co-workers were able to accurately measure the equilibrium constant and subsequently determine the contribution of the destabilizing and stabilizing effects.<sup>8</sup> With AuNPs, however, a two-state model cannot be established and the reported method cannot be directly applied. Nevertheless, we can still conclude that for DNA-linked AuNPs, the excluded volume interaction plays a

major role in the presence of PEG, since an overall increase in  $T_m$  was observed for all the PEGs.

In summary, there are several important conclusions and implications from this study. (1) The effect of PEG on DNA melting is described as the MC effect by biochemists and biophysicists. In the field of colloidal particle aggregation,<sup>26</sup> the same fundamental interaction is known as the depletion force. We consider that the amplified MC effect observed in this work can also be explained using the attractive depletion force. DNA-functionalized AuNPs thus offer a highly tunable experimental system to bridge these two communities. (2) The change of physical property as a function of nanoparticle size is a hallmark of nanoscience. Most of the previous work focused only on properties such as light absorption, emission, phase transition, and melting.<sup>11,27</sup> We show here that the simple geometric interaction can also have a strong nanoscale effect. (3) We may not even need to have large biomolecules to observe the MC effect; even small molecules can be turned into macromolecules as long as they are attached to nanoparticles. The 12-mer DNA is, by itself, considered a small molecule in terms of the crowding effect. It did not show a significant change in the excluded volume upon melting, but the crowding effect was observed when functionalized to AuNPs. (4) DNA-functionalized nanomaterials have already been used as analytical probes and drug carriers.<sup>28</sup> This study indicated that the property of DNA is affected by AuNPs. Therefore, related MC effect needs to be taken into consideration, especially for cellular applications. (5) This study provides a useful means to stabilize weak interactions. By attaching a large number of molecules to nanoparticles in a crowded environment, weak individual interactions may still lead to stable interactions between nanoparticles because of both polyvalent binding and the enhanced MC effect.

## ■ ASSOCIATED CONTENT

### Supporting Information

Materials and methods, geometric calculations, TEM micrographs, UV/vis spectra. This material is available free of charge via the Internet at <http://pubs.acs.org>.

## ■ AUTHOR INFORMATION

### Corresponding Author

liujw@uwaterloo.ca

## ■ ACKNOWLEDGMENTS

This work is supported by the University of Waterloo, Canada Foundation for Innovation, Ontario Ministry of Research and Innovation (Early Researcher Award to J. Liu), and the Natural Sciences and Engineering Research Council (NSERC) of Canada. We thank Dr. Jean Duhamel and the anonymous reviewers for insightful comments and suggestions.

## ■ REFERENCES

- (1) Zimmerman, S. B.; Minton, A. P. *Annu. Rev. Biophys. Biomol.* **1993**, *22*, 27.
- (2) Minton, A. P. *J. Biol. Chem.* **2001**, *276*, 10577. Ellis, R. J. *Trends Biochem. Sci.* **2001**, *26*, 597. Zhou, H.-X.; Rivas, G.; Minton, A. P. *Annu. Rev. Biophys.* **2008**, *37*, 375. Miyoshi, D.; Sugimoto, N. *Biochimie* **2008**, *90*, 1040.
- (3) Woolley, P.; Wills, P. R. *Biophys. Chem.* **1985**, *22*, 89. Miyoshi, D.; Matsumura, S.; Nakano, S.-i.; Sugimoto, N. *J. Am. Chem. Soc.* **2003**, *126*, 165. Miyoshi, D.; Karimata, H.; Sugimoto, N. *J. Am. Chem. Soc.*

- 2006**, *128*, 7957. Smith, B. D.; Liu, J. *J. Am. Chem. Soc.* **2010**, *132*, 6300.
- (4) Spink, C. H.; Chaires, J. B. *Biochemistry* **1999**, *38*, 496.
- (5) Goobes, R.; Kahana, N.; Cohen, O.; Minsky, A. *Biochemistry* **2003**, *42*, 2431.
- (6) Karimata, H.; Nakano, S.; Sugimoto, N. *Bull. Chem. Soc. Jpn.* **2007**, *80*, 1987.
- (7) Nakano, S.-i.; Karimata, H.; Ohmichi, T.; Kawakami, J.; Sugimoto, N. *J. Am. Chem. Soc.* **2004**, *126*, 14330.
- (8) Knowles, D. B.; LaCroix, A. S.; Deines, N. F.; Shkel, I.; Record, M. T. *Proc. Natl. Acad. Sci. U.S.A.* **2011**, *108*, 12699.
- (9) Mirkin, C. A.; Letsinger, R. L.; Mucic, R. C.; Storhoff, J. J. *Nature* **1996**, *382*, 607.
- (10) Alivisatos, A. P.; Johnsson, K. P.; Peng, X.; Wilson, T. E.; Loweth, C. J.; Bruchez, M. P. Jr; Schultz, P. G. *Nature* **1996**, *382*, 609.
- (11) Elghanian, R.; Storhoff, J. J.; Mucic, R. C.; Letsinger, R. L.; Mirkin, C. A. *Science* **1997**, *277*, 1078.
- (12) Storhoff, J. J.; Lazarides, A. A.; Mucic, R. C.; Mirkin, C. A.; Letsinger, R. L.; Schatz, G. C. *J. Am. Chem. Soc.* **2000**, *122*, 4640. Jin, R.; Wu, G.; Li, Z.; Mirkin, C. A.; Schatz, G. C. *J. Am. Chem. Soc.* **2003**, *125*, 1643. Harris, N. C.; Kiang, C. H. *J. Phys. Chem. B* **2006**, *110*, 16393. Smith, B. D.; Dave, N.; Huang, P.-J. J.; Liu, J. *J. Phys. Chem. C* **2011**, *115*, 7851.
- (13) Goodrich, G. P.; Helfrich, M. R.; Overberg, J. J.; Keating, C. D. *Langmuir* **2004**, *20*, 10246.
- (14) Lytton-Jean, A. K. R.; Mirkin, C. A. *J. Am. Chem. Soc.* **2005**, *127*, 12754.
- (15) You, Y.; Tataurov, A. V.; Owczarzy, R. *Biopolymers* **2011**, *95*, 472.
- (16) Jin, R.; Wu, G.; Li, Z.; Mirkin, C. A.; Schatz, G. C. *J. Am. Chem. Soc.* **2003**, *125*, 1643.
- (17) Pramanik, S.; Nakamura, K.; Usui, K.; Nakano, S.-i.; Saxena, S.; Matsui, J.; Miyoshi, D.; Sugimoto, N. *Chem. Commun.* **2011**, *47*, 2790.
- (18) Zwanikken, J. W.; Guo, P.; Mirkin, C. A.; Olvera de la Cruz, M. *J. Phys. Chem. C* **2011**, *115*, 16368.
- (19) Anderson, C. F.; Record, M. T. *Annu. Rev. Phys. Chem.* **1995**, *46*, 657.
- (20) Kuga, S. *J. Chromatogr. A* **1981**, *206*, 449.
- (21) Brandrup, J.; Immergut, E. H.; Grulke, E. A.; Abe, A.; Bloch, D. R. *Polymer Handbook*; Wiley: New York, 2005.
- (22) Park, S. Y.; Lytton-Jean, A. K. R.; Lee, B.; Weigand, S.; Schatz, G. C.; Mirkin, C. A. *Nature* **2008**, *451*, 553.
- (23) Nykypanchuk, D.; Maye, M. M.; van der Lelie, D.; Gang, O. *Nature* **2008**, *451*, 549.
- (24) Park, S. Y.; Lee, J.-S.; Georganopoulou, D.; Mirkin, C. A.; Schatz, G. C. *J. Phys. Chem. B* **2006**, *110*, 12673.
- (25) Spink, C. H.; Garbett, N.; Chaires, J. B. *Biophys. Chem.* **2007**, *126*, 176.
- (26) Park, K.; Koerner, H.; Vaia, R. A. *Nano Lett.* **2010**, *10*, 1433.
- (27) Alivisatos, A. P. *Science* **1996**, *271*, 933.
- (28) Rosi, N. L.; Mirkin, C. A. *Chem. Rev.* **2005**, *105*, 1547. Rosi, N. L.; Giljohann, D. A.; Thaxton, C. S.; Lytton-Jean, A. K. R.; Han, M. S.; Mirkin, C. A. *Science* **2006**, *312*, 1027. Liu, J.; Cao, Z.; Lu, Y. *Chem. Rev.* **2009**, *109*, 1948. Katz, E.; Willner, I. *Angew. Chem., Int. Ed.* **2004**, *43*, 6042. Wang, H.; Yang, R. H.; Yang, L.; Tan, W. H. *ACS Nano* **2009**, *3*, 2451. Zhao, W.; Brook, M. A.; Li, Y. *ChemBiochem* **2008**, *9*, 2363. Ricci, F.; Lai, R. Y.; Heeger, A. J.; Plaxco, K. W.; Sumner, J. J. *Langmuir* **2007**, *23*, 6827. Zhao, C.; Ren, J. S.; Qu, X. G. *Chem.—Eur. J.* **2008**, *14*, 5435.